Testing the hydrological performance of live pole drains (LPD) for mitigation of slope instability

Berlitz, Fernanda; Benschop, Eefje; Mickovski, Slobodan B.; Gonzalez-Ollauri, Alejandro

DOI
10.1016/j.ecoleng.2024.107360

Publication date
2024

Document Version
Final published version

Published in
Ecological Engineering

Ecological Engineering 208 (2024) 107360

Contents lists available at ScienceDirect

Ecological Engineering

journal homepage: www.elsevier.com/locate/ecoleng

Testing the hydrological performance of live pole drains (LPD) for mitigation of slope instability

Fernanda Berlitz [a,*], Eefje Benschop [b], Slobodan B. Mickovski [a], Alejandro Gonzalez-Ollauri [a]

[a] School of Computing Engineering and Built Environment, Department of Civil Engineering and Environmental Management, Glasgow Caledonian University, Cowcaddens Road, G4 0BA Glasgow, UK

[b] Section Water Resources, Department of Water Management, Faculty of Civil Engineering and Geosciences, Delft University of Technology, P.O. Box 5048, 2600 GA Delft, The Netherlands

ARTICLE INFO

Keywords:
Live fascines
Slope stability
Runoff mitigation
Soil-water mass balance
Erosion
Landslides
Laboratory investigation
Soil-plant-atmosphere interaction

ABSTRACT

Nature-based solutions (NbS) and soil bioengineering techniques have gained considerable attention due to their relevant hydrological functions and ability to mitigate slope instability. Live pole drains (LPD), a lesser-known NbS, have traditionally been deployed on slopes to drain the excess surface water and regulate the soil's water budget, making it a suitable technique for stormwater management and landslide prevention. However, neither the LPD performance as a plant-based drainage system nor its potential to regulate the soil-water budget through hydrological processes have been thoroughly studied. This paper presents a novel pilot, lab-based approach for testing the hydrological performance of LPD under different soil hydrological conditions. We built three different treatments and investigated their hydrological performance under multiple storm events. We explored how LPD regulate the soil-water budget by partitioning the water inputs (i.e., rainfall precipitation) into water outputs (i.e., surface runoff, subsurface flow, and percolation). The study revealed that LPD can effectively manage stormwater by draining excess runoff and buffering water in the soil, outperforming fallow soil. Subsurface flow and percolation were significantly higher under LPD treatments when compared to fallow ground, suggesting that the presence of an enhanced structure in the soil results in high soil hydrological performance. The presence of a secondary species with the LPD showed a more efficient hydrological performance than an LPD alone, which aligns with the current implementation of NbS fostering biodiversity. Antecedent soil moisture impacted the hydrological performance of LPD by altering the relative infiltration capacity of the soil and by potentially modifying the availability of channels for preferential flow. Our findings provide a sound basis for future research to improve our understanding of the hydrological performance of LPD for slope instability mitigation and encourage their reproduction and upscaling.

1. Introduction

Climate change has been leading to the intensification and increased frequency of storms. These heavy and prolonged rainfall events will likely increase soil-water saturation and decrease soil shear strength, leading to slope instability and landslides (Sidle and Bogaard, 2016; Gonzalez-Ollauri and Mickovski, 2017a, 2017b) and their associated impact on human life and property. As such, it is essential to devise effective slope drainage and stability approaches. Traditional civil engineering techniques for slope stability and drainage (e.g., retaining walls, piling, shortcreting, piped or channelled slope drainage) are not flexible enough to adapt to climate and environmental changes. Approaches that work with nature (e.g., vegetation) whilst incorporating well-established geotechnical principles, such as soil bioengineering techniques (Schiechtl and Stern, 1997) and related Nature-based Solutions (NbS; e.g., Gonzalez-Ollauri et al., 2023) are feasible, self-repairing, resilient, ecologically functional, and normally more efficient and cheaper than grey infrastructure (Mickovski, 2021). Hence, these solutions are suitable for slope adaptation to climate changes whilst sustainably managing landslides.

The role of vegetation in mitigating rainfall-induced landslides is widely recognised, particularly through soil bioengineering techniques (Stokes et al., 2014). This approach integrates live and dead plant components into the soil, providing mechanical support and acting as

* Corresponding author.
E-mail address: fernanda.berlitz@gcu.ac.uk (F. Berlitz).

https://doi.org/10.1016/j.ecoleng.2024.107360
Received 22 January 2024; Received in revised form 12 May 2024; Accepted 23 July 2024
Available online 22 August 2024

hydraulic drains (Gray and Sotir, 1996). While roots can bond particles through root exudates and microbiological activity, thus increasing soil shear strength and stability (Mickovski and van Beek, 2009; Gonzalez-Ollauri and Mickovski, 2016), the presence of vegetation can facilitate soil-water removal through evapotranspiration, improving infiltration and subsurface flow (Liu et al., 2016; Gonzalez-Ollauri and Mickovski, 2017a; Kim et al., 2017). This helps to balance the soil-plant-atmosphere continuum, leading to a more stable, unsaturated soil and consequent improvement in soil strength.

In the realm of soil bioengineering, one technique that shows great promise for enhancing drainage and restoring slope landscape is known as live pole drains (LPD; Fig. 1; Polster, 1989; Campbell et al., 2008). Essentially, LPD are a sustainable drainage system that uses fascines – i.e., tied cylindrical bundles of live woody cuttings with re-sprouting properties capable of growing shoots and roots (Schiechtl and Stern, 1997; Sotir and Fischenich, 2001). Live fascines are combined with dead bundles, which provide decaying material to improve soil structure and support live bundle development (Norris et al., 2008). All fascines are arranged in a linear or herringbone pattern trench to promote effective subsurface water flow.

LPD increase surface permeability, which allows stormwater runoff to permeate within the soil, taking over surface runoff volume and peak flow (Campbell et al., 2008). With bundles creating a higher number of macropores within the LPD-soil matrix, water subsurface flow increases through preferential flow (Bouma, 1981), resulting in better percolation and drainage performance. Additionally, evapotranspiration is a process acting as a forcing function in removing excess water during the vegetative season, resulting in a balanced soil-water condition (Rodriguez-Iturbe and Porporato, 2005). While a few studies analysed the mechanical potential of live fascines to protect, stabilise and restore riverbanks (Li et al., 2006; Recking et al., 2019), a lack of research and evidence exists regarding LPD hydrological performance in runoff mitigation, soil water budget regulation, and ultimately slope stability enhancement. As a result, LPD have limited adoption for slope drainage and stabilisation as well as stormwater management since they are generally unknown by practitioners and researchers.

The aim of this study was to test the hydrological performance of LPD for slope drainage and stormwater management. A novel laboratory, pilot test with three different treatments (i.e., a willow LPD; a willow with alfalfa LPD; and fallow soil as control) was carried out to quantify hydrological processes by which LPD may improve soil drainage, reduce surface runoff, and thus provide more strength to the soil on the slope. The hydrological processes considered herein were surface runoff, percolation, and subsurface flow. The hydrological performance of LPD was quantified by partitioning the water inputs from rainfall storm simulations into water outputs through water mass balances, while the soil-water dynamics (i.e., volumetric soil moisture, matric suction, and soil temperature) were monitored to explore hydrological changes in the LPD over time. Through our investigation into the LPD effectiveness for slope drainage and stormwater management, our evidence-based findings will support the adoption and upscaling of this NbS, particularly in mitigating the risks associated with slope instability.

2. Materials and methods

2.1. LPD concept model

We built a concept model to capture the hydrological processes occurring at the soil-plant-atmosphere interface in the LPD (Fig. 1b). The concept model, which was built according to well-established ecological and hydrological modelling principles (e.g., Jørgensen and Fath (2011) and Shaw et al. (2017)), integrates LPD features and attributes described in Schiechtl and Stern (1997) and Norris et al. (2008), and the hydrological effects of vegetation on slope stability discussed in Gonzalez-Ollauri and Mickovski (2017a, 2017b). The control volume is defined by the LPD, which comprises a shallow drainage trench, bundles of live plant fascines and their growing root systems, as well as porous, inert earth materials filling the trench. The water inputs (rainfall simulations) and outputs (percolation, subsurface flow, and surface runoff) represent the driving functions of the model. The state variables are represented by the total volumetric water content in the control volume, matric suction, and soil temperature.

2.2. LPD pilot test setup

An LPD pilot test setup was built at Glasgow Caledonian University's Geotechnics laboratory following the LPD concept model (Fig. 1b), and descriptions of live drainage featured in Norris et al. (2008). We built a total of 9 experimental repeats with three different treatments: three basket willow (*Salix viminalis* sp.) and natural soil LPD (W); three basket willow with alfalfa (*Medicago sativa* sp.; seeds, 100 g m^{-2}) and natural soil LPD (W + A); and three unvegetated (fallow) permeable drainages built using natural soil only as control (C). Basket willow was selected for its resilience and fast growth in waterlogged areas, making it a popular choice for soil-bioengineering techniques (Schiechtl and Stern, 1997). Considering the scale of our experiment, only live woody cuttings were used. We included alfalfa in one of the treatments to mimic field conditions, where weeds grow quicker than willows, and to assess the impact of a secondary species colonisation on the hydrological performance of the LPD. Alfalfa was chosen for its ability to thrive in wet soils and under laboratory settings (Lokhorst et al., 2019) and its role in managing runoff and sediment, contributing to soil-water balance (Yao et al., 2023). To ensure alfalfa germination success, we utilised a high-density seeding method (100 g m^{-2}), which is 50 times more than the standard field practices (Box and Carmona, 2005).

Each experimental repeat consisted of a gutter – PVC pipe spliced half lengthwise (L: 500 mm; W: 115 mm; V: 2.6 L) – perforated to enable vertical percolation (Fig. 2a-b). To this end, thirty-three holes were drilled (∅ 4 mm; 50 mm equidistance between holes) per gutter, following a zig-zag pattern formed by 3 rows in the length of the pipe (Fig. 2a). The central row followed the middle of the gutter, while the two lateral rows (one on each side of the gutter) were drilled at a 30 mm distance from the edge of the gutter. The crests of the gutters were closed with duct tape to avoid soil loss and/or displacement (Fig. 2c). Subsequently, a nylon mesh (L: 600 mm; W: 200 mm; mesh size: 20 μm) was placed inside the gutters to avoid loss of fine soil particles from the columns through internal erosion (Fig. 2c-d). The gutters' toes were closed with the same nylon mesh, allowing subsurface flow without losing any soil material (Fig. 2d).

Six bundles of 15 live cuttings of basket willow were created for the W and W + A LPD treatments (Fig. 3). The cuttings were collected from healthy adult individuals in Catterline Bay, Aberdeenshire, UK, during the vegetative season of 2022. The live cuttings were preserved by submerging them in clean freshwater up to 80% of their length before being assembled into bundles. Each cutting was clipped to a length of 450 mm (Fig. 3a-b). The diameter of each cutting was measured using Vernier callipers and sorted into ten groups based on their diameter ranging from ∅ 3 mm to ∅ 12 mm. The cuttings were then grouped into bundles of 15 cuttings each, striving for a balanced distribution according to their diameter and assembled in the same direction – i.e., all the tips of live cuttings were to be positioned at the toe of the column to promote adequate drainage (Schiechtl and Stern, 1997; Campbell et al., 2008). The bundles were created to achieve a similar branch size distribution (average macropore fraction 58%), circumference (average bundle ∅ 37.8 mm) and volume (average bundle V: 0.5 L). Eventually, the bundles were tightly tied with gardening twine at 100 mm from each end (Fig. 3c) and placed in a bucket of water until they could be placed into the drainage trench.

Six out of nine gutters received a first layer of silty sand soil (Sand: 79.82%; Silt: 5.85%; Clay: 3.08%; Gonzalez-Ollauri and Mickovski, 2017a), which was collected from the same site as the willow cuttings. Prior to this, the soil was air-dried for 4 to 6 days with additional oven

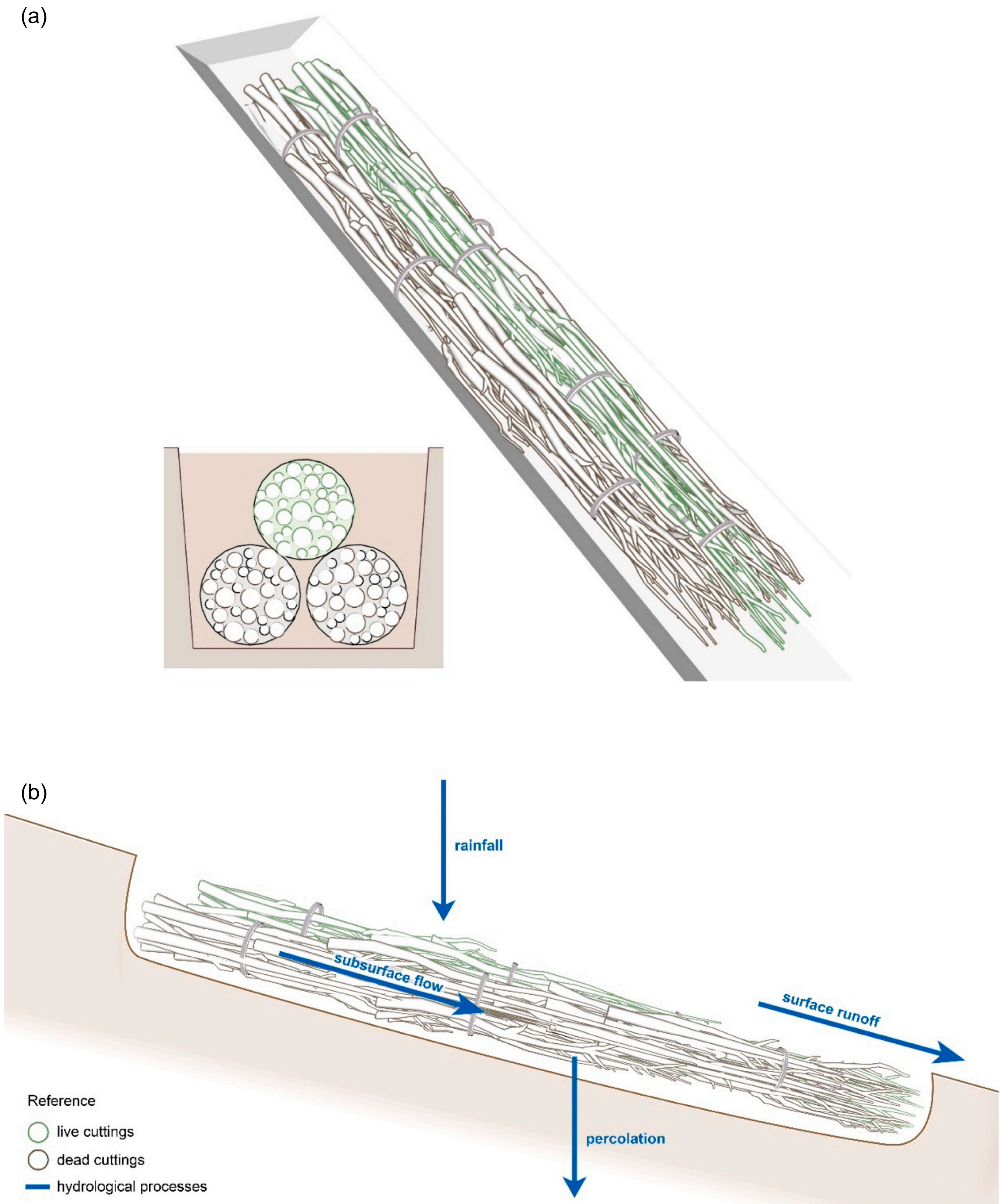

Fig. 1. Schematic drawings of Live pole drains. (a) Plan view and cross-section of LPD following design guidelines by Campbell et al. (2008) and Norris et al. (2008); (b) LPD longitudinal view and conceptual model, where the hydrological processes represent the water fluxes within an LPD, also connecting atmosphere, above- and belowground vegetation, and soil compartments.

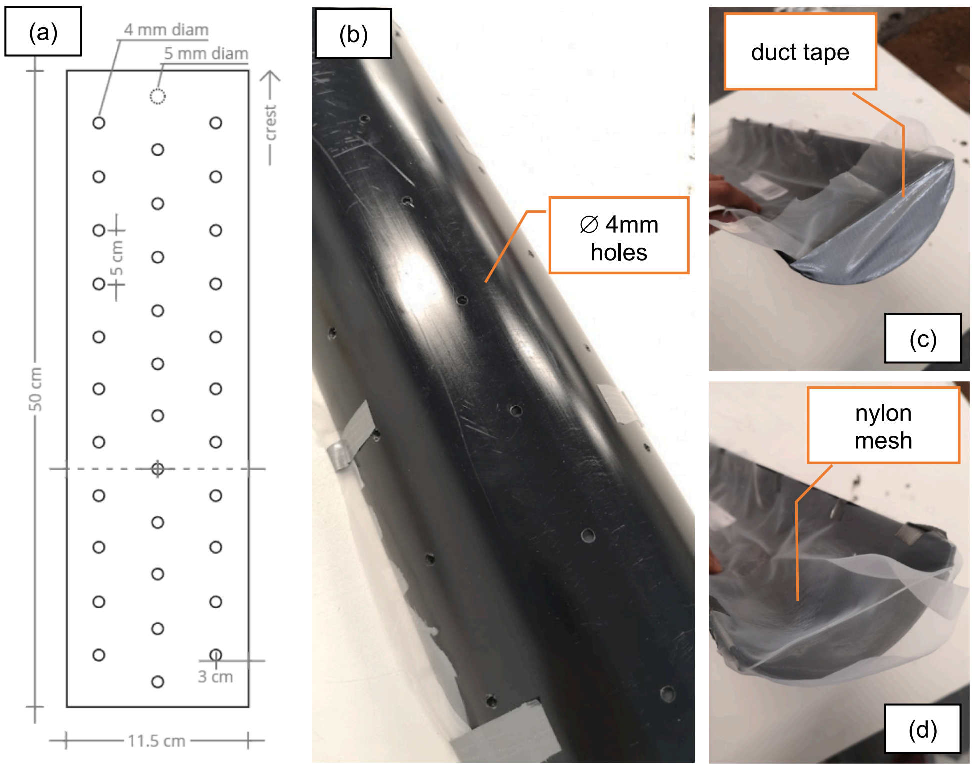

Fig. 2. Steps to build the columns (Part 1). (a) Sketch illustrating gutter dimensions and positioning of drilled holes allowing vertical percolation; (b) Perforated gutter; (c) Crest of column closed with duct tape avoiding soil loss; (d) Nylon mesh applied to avoid loss of soil fines and to allow data collection on subsurface flow.

drying at 100 °C for 24 h. Once dried, the soil was pulverised with a pestle and sieved through a 2 mm sieve, removing all stones and gravel from the bulk soil sample. Once the soil was added to the gutter, it was gently compacted by hand. Then, a groove (i.e., infiltration trench) was created, and one willow bundle was placed inside (Fig. 3d). Subsequently, the groove and bundle were covered with soil material and gently compacted by hand to achieve a low bulk density of ca. 0.76 g/ cm^3 (bulk density similar to porous soils with organic matter, ranging from 0.8 to 0.9 g/cm^3; Panagos et al., 2024) to avoid any possible root growth obstructions and allow high soil permeability (Fig. 3e-f). On average, the willow bundle occupied 19.5% of the total gutter volume. LPD under the W + A treatment were sown with alfalfa seeds with a density of 100 g m^{-2} (Fig. 3g). In the control columns (C), gutters were filled only with soil and gently compacted to achieve the same bulk density as the LPD. Eventually, a flexible funnel was installed above the soil at the toe of each column (Fig. 3h) to collect surface runoff separately from subsurface flow (Fig. 3h-i). The flexible funnel was installed to convey water that does not infiltrate the soil and results in surface runoff. Four plastic containers of 0.65 L capacity were placed below and at the end of each column to collect percolation (2 containers), subsurface flow (1 container), and surface runoff water (1 container; see Section 2.1 LPD Concept Model).

The experimental setup was placed for 52 days within a growing chamber programmed with a constant mean air temperature of 22 °C and humidity of 80% (Fig. 4). Each gutter was tilted at 30° and placed under artificial sunlight between 6 AM and 10 PM (14 h day^{-1}; irradiance 165 W m^{-2}; Spider Farmer SF2000) to stimulate vegetation growth. Daily monitoring of willow development was conducted to measure the number and height of new resprouting stems by placing a ruler against the stem.

Lastly, constant irrigation with an average of 3.56 mm h^{-1} of water per treatment was supplied with a drip irrigation system to stimulate plant growth. To this end, an irrigation system (Fig. 5a) was created by modifying a garden dripping system and adjusted to provide a constant water supply to the columns. Two dripping nozzles were placed 100 mm above the ground at an equal distance along each gutter. Water was sourced from three 25 L water tanks (one for every 3 columns; Fig. 5a). The system was calibrated by opening the connected water tank and adjusting the nozzles to achieve an equal irrigation rate. This resulted in one drop of water every 4 s.

2.3. *Storm simulation*

A portable rainfall simulator was built using three irrigation drip nozzles (H: 33 mm; ∅ 15 mm), with one nozzle per treatment and a supporting frame made with bamboo dowels (Fig. 5b). The frame consisted of three vertical dowels spaced equally to fit a gutter in between. The horizontal dowel held the nozzles at a height of 200 mm above the ground level at the crest of the column. The water supply for the storm simulations was done through a water tap to achieve higher water flow and pressure. The storm simulator was calibrated by measuring the water volume released by each nozzle ten times for one minute each. On average, each nozzle discharged 0.31 L min^{-1}, equivalent to a rainfall event of 372.72 mm h^{-1} per gutter area.

Different storm events were simulated after 20 days of setup deployment and plant development. Five storm events were designed with varying durations and distributions (Table 1), following an intensity-duration-frequency (IDF) model (UKCEH, 1999), with an additional 30% over rainfall intensity as an effect of climate change (Scottish Water, 2018). Each rainfall (RF) event was distributed differently to mimic natural conditions in which rainfall depth and intensity are distributed unevenly over the storm duration (Shaw et al., 2017).

Each storm simulation was performed at least twice: the first simulation was carried out four hours after closing the irrigation system with soil at a high-water saturation level (scenario A; ScA). The second simulation was carried out 24 h later, with soil at its field capacity (scenario B; ScB).

Fig. 3. Steps to build the LPD columns (Part 2). (a) Initial assembly of live cuttings and health assessment; (b) Live cuttings clipped and grouped together, striving a similar bundle diameter; (c) Tied bundles at 100 mm of each end; (d) Bundle placed in the groove made in the soil column; (e) Sides of the bundle being covered with soil; (f) Total bundle coverage; (g) Sown alfalfa seeds under the W + A treatment; (h) Flexible funnel installed above the soil at the toe of each column to allow surface runoff collection; (i) Container placed below the flexible funnel to allow water collection of subsurface flow.

2.4. Soil-water mass balance (SWMB)

The soil-water mass balance (SWMB) was calculated to evaluate the hydrological performance of LPD (Eq. 1). Eq. 1 shows how water inputs (i.e., the combined volume of rainfall) were distributed into water outputs (i.e., the combined volumes of surface runoff, subsurface flow, and percolation). Additionally, the LPD potential to retain water was assessed by quantifying the difference in soil-water content pre- and post-storm simulation. The SWMB also included a term for water loss to refer to any potential losses and errors produced in the simulation of

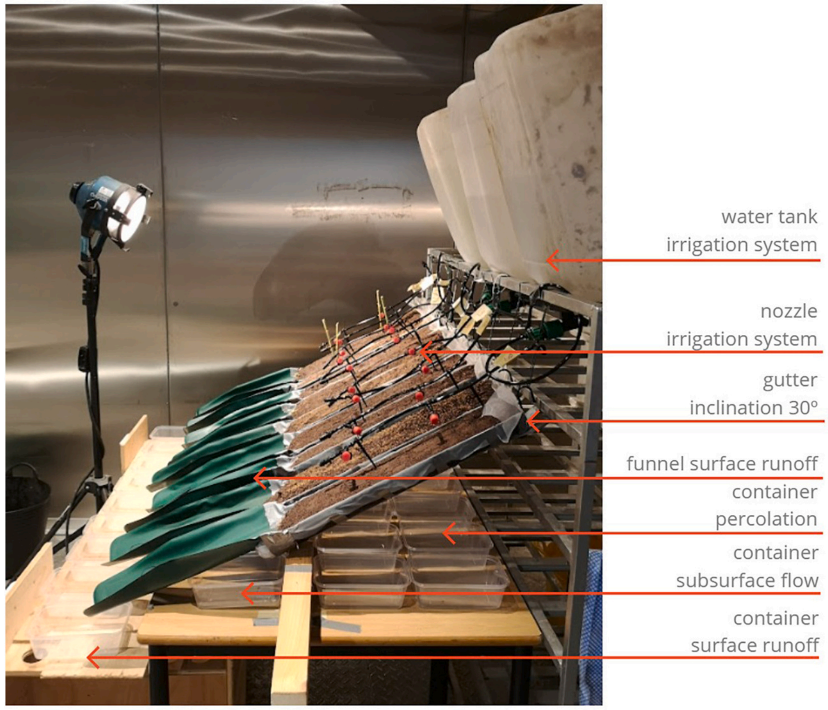

Fig. 4. Lateral view of the LPD pilot test setup and its main components.

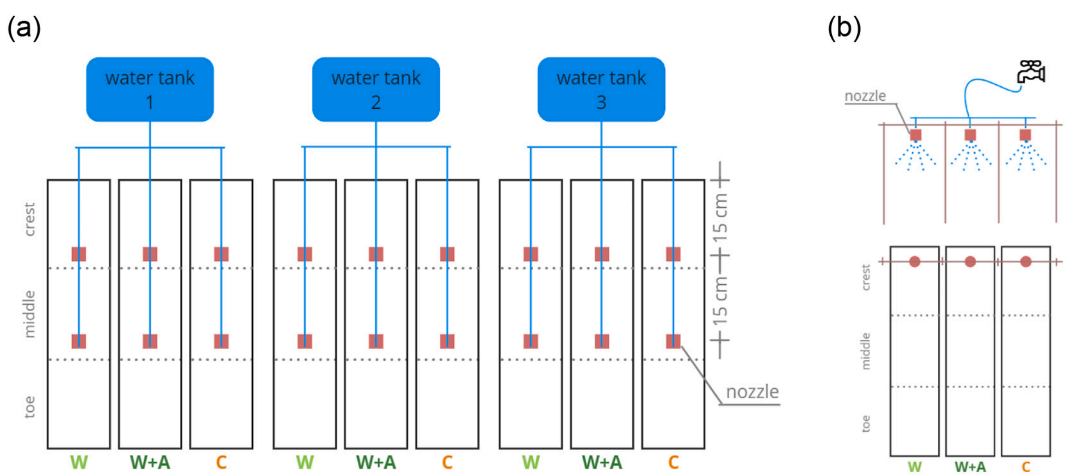

Fig. 5. (a) Sketch illustrating the irrigation system built to provide constant water supply to treatments and foster plant growth; (b) Sketch illustrating the rainfall simulator.

rainfall that were not captured upon measuring water volume partitioned for each considered hydrological process.

$$[CWV] = [SR + SF + P] + [WC_a - WC_b] + [W_\ell] \quad (1)$$

Where:
CWV = Cumulative water volume, in litres.
SR = Surface runoff, in litres.
SF = Subsurface flow, in litres.
P = Percolation, in litres.
WC_a = Water content in soil – after rainfall, in litres.
WC_b = Water content in soil – before rainfall, in litres.
W_ℓ = Water loss, in litres.

Water volumes resulting from surface runoff, subsurface flow, and percolation processes were measured 30 min after each simulated storm (see Section 2.3 Storm Simulation). The water volume collected in each of the different plastic containers placed under and at the end of the experimental setup (Fig. 4; see Section 2.2 LPD Pilot Test Setup) was measured with a 1000 mL graduated cylinder. The soil-water retention was estimated by calculating the difference in soil volumetric water content (θ; %) measured before and after the simulated storm. The volumetric water content (θ; %) was subsequently converted to litres based on the soil bulk density, soil porosity, and total pore-water volumes.

2.5. Soil-water dynamics

We continuously measured volumetric soil moisture content (θ), soil matric suction (φ), and soil temperature (t) for 30 days during wetting soil conditions (i.e., with irrigation or simulated rainfall) and drying soil conditions (i.e., without irrigation or simulated rainfall). We considered these soil-water variables to supplement the Soil-Water Mass Balance

Table 1
Storm simulations performed during the laboratory experiment. RF: rainfall.

Storm Simulation	Total Duration (min)	Type of Rainfall	Rainfall Intensity (mm h^{-1})	Return Period Equivalent (years)	Cumulative Water Volume (CWV; L)
RF 1	1	1 interval of 1 min	372.72	1:1000	0.31
RF 2	14	7 intervals of 1 min; pauses of 1 min	186.36	1:200	2.20
RF 3	10	10 intervals of 30 s; pauses of 30 s	93.18	1:25	1.57
RF 4	15	3 intervals of 1 min; pauses of 4 min	74.54	1:10	0.94
RF 5	14	2 intervals of 2 min; pauses of 5 min	106.49	1:100	1.26

(SWMB; Eq. 1; Fig. 1b). Soil-water dynamics were measured with pre-calibrated, automatic sensors installed two weeks after the first willow LPD resprouted (day 18). The sensors were inserted vertically in the middle of the column and as close to the LPD bundle as possible. We used six soil moisture sensors (two sensors per treatment; SEN0193 – DF Robot), three tensiometers (one sensor per treatment; T5 – UMS) and nine temperature probes (three sensors per treatment; 107 – Campbell Scientific) wired to an electric-powered data logger (CR1000 – Campbell Scientific), which collected records every 5 min. Time series for soil-water variables were integrated into hourly time steps.

2.6. Statistical data analysis

Normal distribution checks of the data retrieved during the experiment (i.e., percolation volume, subsurface volume, surface runoff volume, volumetric soil moisture content, matric suction, and soil temperature) were performed with Shapiro-Wilk tests. If the data did not follow a normal distribution, a non-parametric test was selected to analyse the statistical differences between experimental treatments. The Kruskal-Wallis test (H) was used to identify statistical differences at the 95% and 99% confidence levels regarding the soil-water mass balance between treatments and scenarios (Kruskal and Wallis, 1952). Additionally, further statistical analysis was conducted by plotting the cumulative distribution functions (CDF) to investigate statistically significant differences between the time series by examining the distance between density functions as an indicator of differences (See Supplementary Material). Statistically significant differences were evaluated with the Kolmogorov-Smirnov test (K-S; Pratt and Gibbons, 1981) at the 95% and 99% confidence levels. All statistical analyses were conducted using the statistical computing software R v4.1.1.

3. Results

3.1. Plant development

The LPD pilot experiment yielded 136 resprouting willow stems, with 71 new willows growing under the willow LPD (W) treatment and 65 new individuals observed within the willow with alfalfa LPD (W + A). However, no statistically significant differences were found in new aboveground vegetation growth between treatments ($H = 0.43$, $df = 1$, $p = 0.51$). Table 2 and Fig. 6 show the aboveground development of the willow stems observed on days 3, 10, 20, 36, and 50, with the highest count number of live new willows found on day 24 ($n = 129$) and the tallest willow observed on day 50 (height = 722.0 mm).

3.2. Soil-water mass balance (SWMB)

Fig. 7 and Table 3 display the results of the Soil-Water Mass Balance (SWMB) components – i.e., surface runoff, subsurface flow, percolation, water retention, and water loss.

In terms of water volume per unit area (L m^{-2}; Fig. 7; Table 3), subsurface flow and percolation were, on average, 1.7 and 1.5 times higher, respectively, in the willow with alfalfa LPD (W + A) treatment compared to fallow soil (C). In contrast, surface runoff under the W + A treatment was, on average, 0.9 times lower than the C treatment. In the case of the willow LPD (W) treatment, subsurface flow and percolation were, on average, 1.4 and 0.4 times higher, respectively, compared to fallow soil (C). Surface runoff under W treatment was, on average, 0.8 times lower than in C. Regarding water retention, both vegetated treatments (W + A and W) were, on average, 0.5 times lower than fallow soil (C) in terms of water volume per unit area (L m^{-2}).

Statistically significant differences were noted between the three treatments (Fig. 7). Among the SWMB components, surface runoff (Fig. 7a; $H = 36.23$, $df = 2$, $p < 0.01$), subsurface flow (Fig. 7b; $H = 17.88$, $df = 2$, $p < 0.01$), and percolation (Fig. 7c; $H = 11.60$, $df = 2$, $p < 0.01$) showed substantial differences between the three soil covers. Although water retention was different between the three treatments (Fig. 7d), it was not as statistically significant as in the other SWMB components ($H = 5.22$, $df = 2$, $p = 0.07$). Water loss significantly differed between treatments (Fig. 7e; $H = 13.00$, $df = 2$, $p < 0.01$).

Surface runoff under fallow soil (C) accounted for up to 19.0% of the total water input (L m^{-2}; Table 3), while willow LPD (W) and willow with alfalfa LPD (W + A) summed up to 6.1% and 2.3% of the total water input, respectively (L m^{-2}; Table 3). Surface runoff was statistically significantly higher in fallow soil (C) than in the vegetated treatments under both scenarios (Fig. 7a; W(ScA): $D = 0.67$ $p < 0.01$; W(ScB): $D = 0.80$ $p < 0.01$; W + A(ScA): $D = 0.73$ $p < 0.01$; W + A(ScB): $D = 0.80$ $p < 0.01$). When comparing the two vegetated treatments against each other, the observed surface runoff was not statistically significantly different (Fig. 7a; ScA: $D = 0.47$ $p = 0.08$; ScB: $D = 0.40$ $p = 0.18$).

Conversely, subsurface flow under willow with alfalfa LPD (W + A; water output up to 32.5% of the total water input; L m^{-2}; Table 3) and willow LPD (W; water output up to 31.2% of the total water input L m^{-2}; Table 3) was significantly higher than the values observed under fallow soil (C; 13.8% of the total water input L m^{-2}; Table 3; Fig. 7b; W(ScA): $D = 0.60$ $p < 0.01$; W(ScB): $D = 0.53$ $p < 0.05$; W + A(ScA): $D = 0.60$ $p < 0.01$; W + A(ScB): $D = 0.60$ $p < 0.01$). Between the vegetated treatments, the found differences were not statistically significant (Fig. 7b; ScA: $D = 0.13$ $p = 1.00$; ScB: $D = 0.20$ $p = 0.94$).

Willow with alfalfa LPD (W + A) showed higher percolation than under willow LPD (W) and fallow soil (C), accounting for up to 44.9%, 25.4%, and 15.3% of the total water input, respectively (L m^{-2}; Fig. 7c; Table 3). The only statistically significant difference for percolation was

Table 2
Aboveground development of the willow stems observed on days 3, 10, 20, 36, and 50.

Day	Count Live Stems	Lowest Stem Height (mm)	Highest Stem Height (mm)	Average Stem Height (mm)
03	9	2.0	25.0	12.6
10	78	2.0	121.0	46.4
20	124	7.0	218.0	109.1
36	120	6.0	433.0	206.6
50	97	24.0	722.0	330.6

Fig. 6. Timeline of willow growth observed during the experiment.

found between the willow with alfalfa LPD (W + A) and fallow soil (C) at scenario A (ScA; Fig. 7c; D = 0.60 $p < 0.01$). At ScA, the observed results were not significantly different between the vegetated treatments (D = 0.47 $p = 0.08$) and between willow LPD (W) and fallow soil (C; D = 0.40 $p = 0.18$). At ScB, vegetated treatments statistically did not differ from fallow soil (C; W: D = 0.20 $p = 0.94$ and W + A: D = 0.40 $p = 0.18$). Between the two LPD (W and W + A), the same pattern was found (Fig. 7c; D = 0.33 $p = 0.39$).

Regarding water retention, the highest volumes per unit area were observed under fallow soil (C; Fig. 7d; Table 3). Water retention under fallow soil (C) accounted for up to 3.5% of the total water input (L m^{-2}; Table 3), while willow LPD (W) and willow with alfalfa LPD (W + A) summed up to 1.3% and 1.7% of the total water input, respectively (L m^{-2}; Table 3). These results were statistically significant only in scenario A (ScA; W(ScA): D = 0.60 $p < 0.01$; W(ScB): D = 0.47 $p = 0.08$; W + A (ScA): D = 0.53 $p < 0.05$; W + A(ScB): D = 0.47 $p = 0.08$). Between the vegetated treatments, the found differences were not significant (ScA: D = 0.47 $p = 0.08$; ScB: D = 0.47 $p = 0.08$).

Water loss under fallow soil (C) accounted for up to 48.4% of the total water input (L m^{-2}; Fig. 7e; Table 3), while willow LPD (W) and willow with alfalfa LPD (W + A) accounted for up to 36.0% and 18.6% of the total water input, respectively (L m^{-2}; Table 3). Water loss was similar across the three treatments and two scenarios (Fig. 7e; Table 3), apart from the values observed between the willow with alfalfa LPD (W + A) and fallow soil (C) at scenario A (ScA; D = 0.60 $p < 0.01$). At ScA, the observed differences were not statistically significant between the vegetated treatments (D = 0.47 $p = 0.08$) and between willow LPD (W) and fallow soil (D = 0.27 $p = 0.68$). At ScB, vegetated treatments statistically did not differ from fallow soil (W: D = 0.20 $p = 0.94$ and W + A: D = 0.33 $p = 0.39$). The same statistical similarity was identified between the vegetated treatments (D = 0.33 $p = 0.39$).

3.3. Soil-water dynamics

3.3.1. Volumetric soil moisture content

The hourly volumetric soil moisture content time series (θ; Fig. 8a) had clear differences between the three treatments. Willow LPD (W) exhibited the highest recorded θ of 44.95% on day 48, while the lowest θ of 27.96% was observed under fallow soil (C) on day 45. Rainfall simulations consistently induced a positive response in θ throughout the experiment (Fig. 8a).

Throughout the observation period, θ under fallow soil (C) consistently remained lower than that under willow LPD (W) and willow with alfalfa LPD (W + A), leading to statistically significant differences between non-vegetated and vegetated treatments (W: D = 0.92 $p < 0.01$; W + A: D = 0.96 $p < 0.01$). Among the vegetated treatments, θ under W + A generally exceeded θ under W until day 46 when this observation shifted. Although vegetated treatments showed similar θ values during the experiment, the differences in θ between vegetated ground covers remained statistically significant (D = 0.32 $p < 0.01$).

The differences in soil moisture content among LPD treatments were more pronounced under drying soil conditions (i.e., without irrigation or simulated rainfall, e.g., θ from day 21 to day 25, from day 36 to day 38, and from day 43 to day 45) than during wetting soil conditions (i.e., with irrigation or simulated rainfall, e.g., θ from day 10 to day 41). An anomaly was observed in the time series, notably the highest recorded θ value of 44.95% observed under willow LPD (W) on day 48.

3.3.2. Soil matric suction

The hourly soil matric suction time series (φ; Fig. 8b) showed clear differences among the three treatments. The highest φ recorded of −90.22 kPa was observed under fallow soil (C) on day 44, while the lowest φ of −0.36 kPa was found under the willow LPD (W) on day 46. Throughout the time series, a negative response of φ to rainfall simulations was consistently noted (Fig. 8b).

Statistically significant φ differences were noted between fallow soil

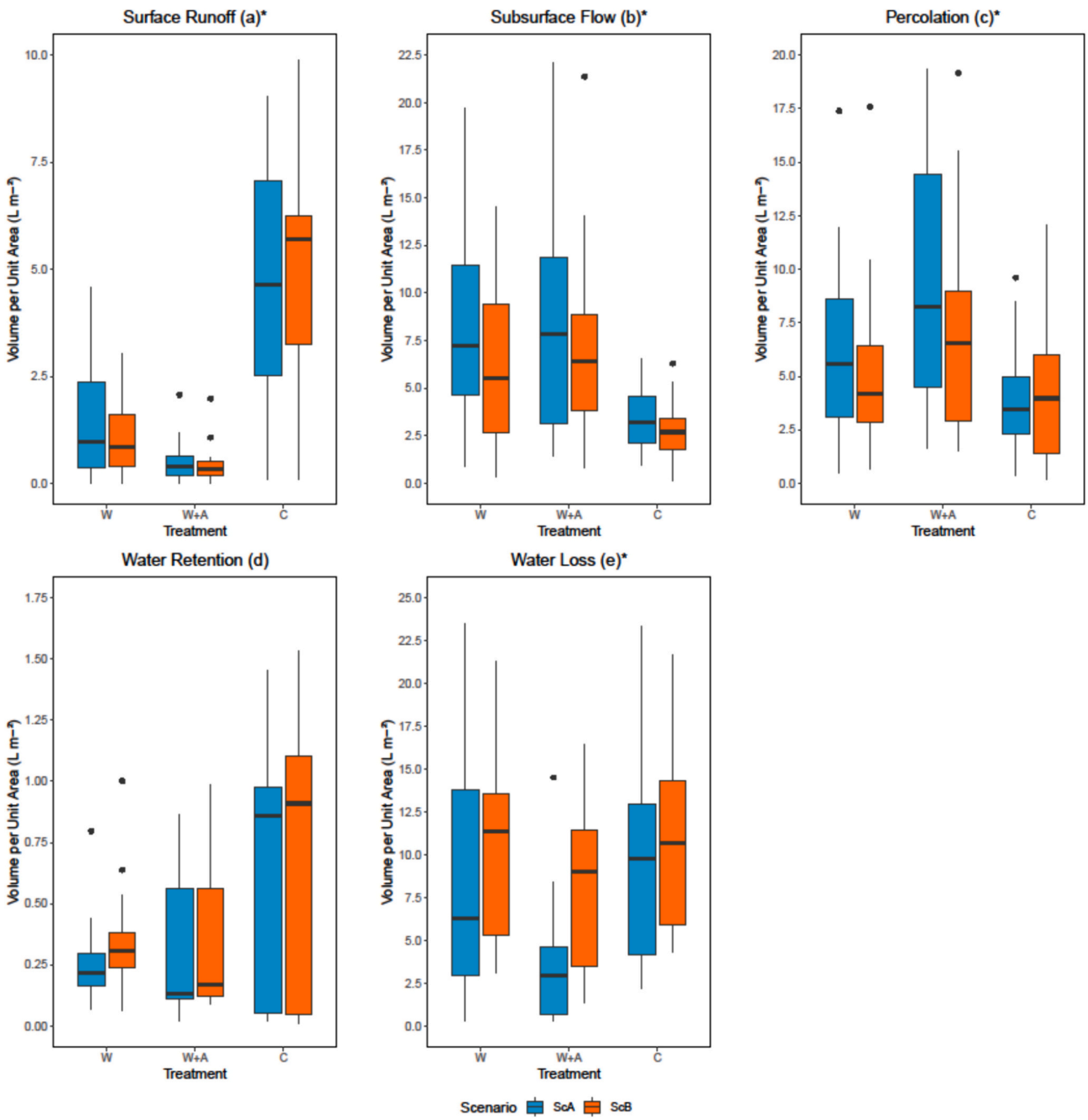

Fig. 7. Box plots for the Soil-Water Mass Balance (SWMB) components. (a) Surface runoff; (b) Subsurface flow; (c) Percolation; (d) Water retention; (e) Water loss. Water volume per unit area (L m^{-2}) under willow LPD (W), willow with alfalfa LPD (W + A), and fallow soil (C) treatments at different scenarios (ScA: soil at water saturation; ScB: soil at field capacity). The lower edge of the box corresponds to the 25th percentile data point, while the top edge of the box corresponds to the 75th percentile data point. The line within the box represents the median.
* 0.01 level significant.

(C) and vegetated treatments (W: $D = 0.12$ $p < 0.01$; W + A: $D = 0.13$ $p < 0.01$). Notably, φ under the willow LPD (W) showed similar behaviour to fallow soil (C) throughout the experiment. This behaviour was not observed when comparing fallow soil (C) with the willow with alfalfa LPD (W + A) treatment, which exhibited the lowest records throughout the observation period.

Between the vegetated treatments, φ under W + A generally registered lower values than φ under W, maintaining significant differences throughout the observation period ($D = 0.14$ $p < 0.01$). Variations in the pattern of φ under the vegetated treatments (W and W + A) were found during the three major drying soil conditions periods (i.e., without irrigation or simulated rainfall, e.g., θ from day 21 to day 25, from day 36 to day 38, and from day 43 to day 45). During the first drying soil conditions period, W exhibited the highest φ, whereas W + A reached −60 kPa. However, these observations were inconsistent during the second and third drying soil conditions periods, wherein fallow soil (C) showed the highest φ values, and W + A recorded φ values below −15 kPa.

3.3.3. Soil temperature

The hourly soil temperature time series (t; Fig. 8c) exhibited distinct differences between treatments. The highest recorded t of 23.27 °C was

Table 3
Summary of hydrological processes making up the Soil-Water Mass Balance (SWMB). Water outputs volumes per unit area (L m^{-2}) and partitioning in relation to water inputs (%) under willow LPD (W), willow with alfalfa LPD (W + A), and fallow soil (C) treatments at different scenarios (ScA: soil at water saturation; ScB: soil at field capacity) by their mean values and range values.

		Willow LPD (W)		Willow with alfalfa LPD (W + A)		Fallow Soil (C)	
		L m^{-2}	%	L m^{-2}	%	L m^{-2}	%
Surface Runoff	mean (ScA)	1.42	6.10	0.51	2.33	4.68	18.96
	range (ScA)	0.00–4.59	0.00–18.48	0.00–2.06	0.00–8.31	0.08–9.04	1.32–42.77
	mean (ScB)	0.99	4.41	0.45	1.68	5.18	19.02
	range (ScB)	0.01–3.03	0.07–16.28	0.01–1.98	0.23–7.96	0.09–10.05	1.44–39.78
Subsurface Flow	mean (ScA)	8.06	31.24	8.63	32.50	3.22	13.83
	range (ScA)	0.89–19.70	14.36–64.67	1.44–22.08	11.54–50.77	0.96–6.52	7.84–19.39
	mean (ScB)	6.18	22.92	7.28	28.62	2.67	10.22
	range (ScB)	0.36–14.56	2.94–46.87	0.80–21.28	12.83–49.15	0.12–6.30	1.91–17.15
Percolation	mean (ScA)	6.36	25.39	11.90	44.86	3.96	15.30
	range (ScA)	0.48–17.39	7.70–41.76	1.62–25.79	21.24–62.35	0.37–9.60	5.88–24.28
	mean (ScB)	5.29	20.11	8.39	31.22	4.16	14.80
	range (ScB)	0.67–17.59	9.99–40.45	1.50–23.91	13.20–56.87	0.19–12.05	3.02–27.72
Water Retention	mean (ScA)	0.25	1.30	0.27	1.74	0.65	3.53
	range (ScA)	0.00–0.80	0.00–3.41	0.00–0.86	0.00–12.08	0.00–1.45	0.00–13.09
	mean (ScB)	0.36	2.46	0.35	2.10	0.69	3.26
	range (ScB)	0.06–1.00	0.14–16.11	0.09–0.98	0.26–10.94	0.01–1.53	0.10–7.05
Water Loss	mean (ScA)	8.76	35.97	3.53	18.57	12.35	48.38
	range (ScA)	0.27–23.49	1.47–57.74	0.28–14.50	1.17–58.36	2.18–32.34	14.38–74.37
	mean (ScB)	12.04	50.10	8.38	36.38	12.14	52.70
	range (ScB)	3.12–25.18	19.43–73.30	1.34–16.46	10.63–63.14	4.31–25.31	26.55–86.69

observed under fallow soil (C) on day 25, while the lowest t of 17.95 °C was noted under the willow LPD (W) on day 19. A consistent negative response of t to rainfall simulations was observed throughout the experiment (Fig. 8c).

Statistically significant differences in t were noted between fallow soil (C) and vegetated treatments (W: $D = 0.27$ $p < 0.01$; W + A: $D = 0.36$ $p < 0.01$). Additionally, t under W + A generally exceeded t under W, showcasing substantial differences throughout the observation period ($D = 0.61$ $p < 0.01$). The time series plots for the three treatments displayed notable fluctuations in t, primarily influenced by artificial daily sunlight provided for plant development. Generally, t remained higher during the day (from 6 am to 10 pm) and decreased during the night (from 10 pm to 6 am).

4. Discussion

The experimental results shown herein indicate that LPD have the potential to effectively manage stormwater on slopes which may experience instability due to extreme rainfall events. Our findings indicate that LPD can successfully drain excess stormwater runoff (Fig. 7), while also effectively buffering water in the soil, outperforming fallow soil (Fig. 8). LPD can control surface water excess, which has the potential to delay peak flows and thus mitigating floods. Through their drainage mechanism, LPD help to stabilize the soil-plant-atmosphere continuum, resulting in a more balanced, unsaturated soil. Additionally, LPD can buffer moisture levels, leading to higher overall moisture content and, thus, higher soil-water availability during drought conditions. Based on these significant findings, LPD can be a viable solution for mitigating slope instability with sustainable slope drainage and stormwater management during rainfall and storm events. Moreover, they can also be a reliable solution for creating water-resilient areas (Scottish Government, 2021) or sponge cities (Zha et al., 2021), further emphasising their effectiveness and multifunctionality.

Substantially lower surface runoff was observed under the LPD compared to fallow soil (Fig. 7a; Table 3). Stormwater likely infiltrated through the root system and enhanced soil structure, leading to more infiltration and percolation, following the findings of Kuehler et al. (2017). Our findings suggest that LPD can also effectively reduce peak flow and thus help mitigate flood risks derived from convective summer storms (Shaw et al., 2017). We also confirm that LPD can be suitable for protecting (before) and restoring (after) slopes and riverbanks prone to landslides and erosion. In this regard, LPD can be a viable technique for non-hardstanding urban areas that still produce substantial stormwater runoff (e.g., gardens, brownfields, road embankments, etc.).

LPD had significantly higher subsurface flow and higher percolation than fallow ground (Fig. 7b-c; Table 3). This is due to the higher number of macropores created by the living cuttings in the bundles and the growing roots, but also due to the likely enhancement of the soil (Ghestem et al., 2011; Gonzalez-Ollauri and Mickovski, 2020). These findings reinforce our working hypothesis that LPD can be an effective NbS for slope drainage and, thus, for managing landslides (Gonzalez-Ollauri and Mickovski, 2017a). The fact that LPD showed substantial subsurface flow volumes suggests that in the event of torrential rainfall, LPD could help increase the lag between the storms and the hydrograph's peaks (Miller et al., 2023), as well as divert the water percolating into the soil towards the drains. These functions of the LPD will give the responsible authorities more response time to act against slope instability and flood events (Fleming, 2002).

Furthermore, the enhanced soil structure within LPD (i.e., bundles of live plant fascines and their growing root systems) leads to lower water retention compared to fallow ground under rainfall conditions (Fig. 7d; Table 3), corroborating with previous findings of Lu et al. (2020) and Zhang et al. (2023). Together with their mechanisms of subsurface flow and percolation, LPD retain less water in soil, promoting a balanced soil-plant-atmosphere continuum, resulting in a stable, unsaturated soil and improved soil strength (Gerten et al., 2004; Liu et al., 2016).

The hydrological response differed between the two vegetated treatments (Fig. 7; Table 3). On average, willow with alfalfa LPD (W + A) cover had lower surface runoff, while subsurface flow, percolation and water retention were significantly higher than willow LPD alone. These outputs can notably be attributed to the presence of a rougher ground surface resulting from the herbaceous ground cover (Guo et al., 2019; Yao et al., 2023). While aboveground vegetation of alfalfa increases soil cover and roughness, thus decreasing surface runoff, belowground alfalfa contributed to opening the soil and creating channels that enhanced preferential flow (Mitchell et al., 1995; Li et al., 2023). In terms of water retention, dense root systems from willow and alfalfa roots (i.e., willow with alfalfa LPD; W + A) likely enlarged the extent of the rhizosphere and the amount of micropores (Bodner et al., 2014), increasing the number of points where water can be held within the soil matrix. These findings indicate that the hydrological performance of LPD can improve when combined with other plant species,

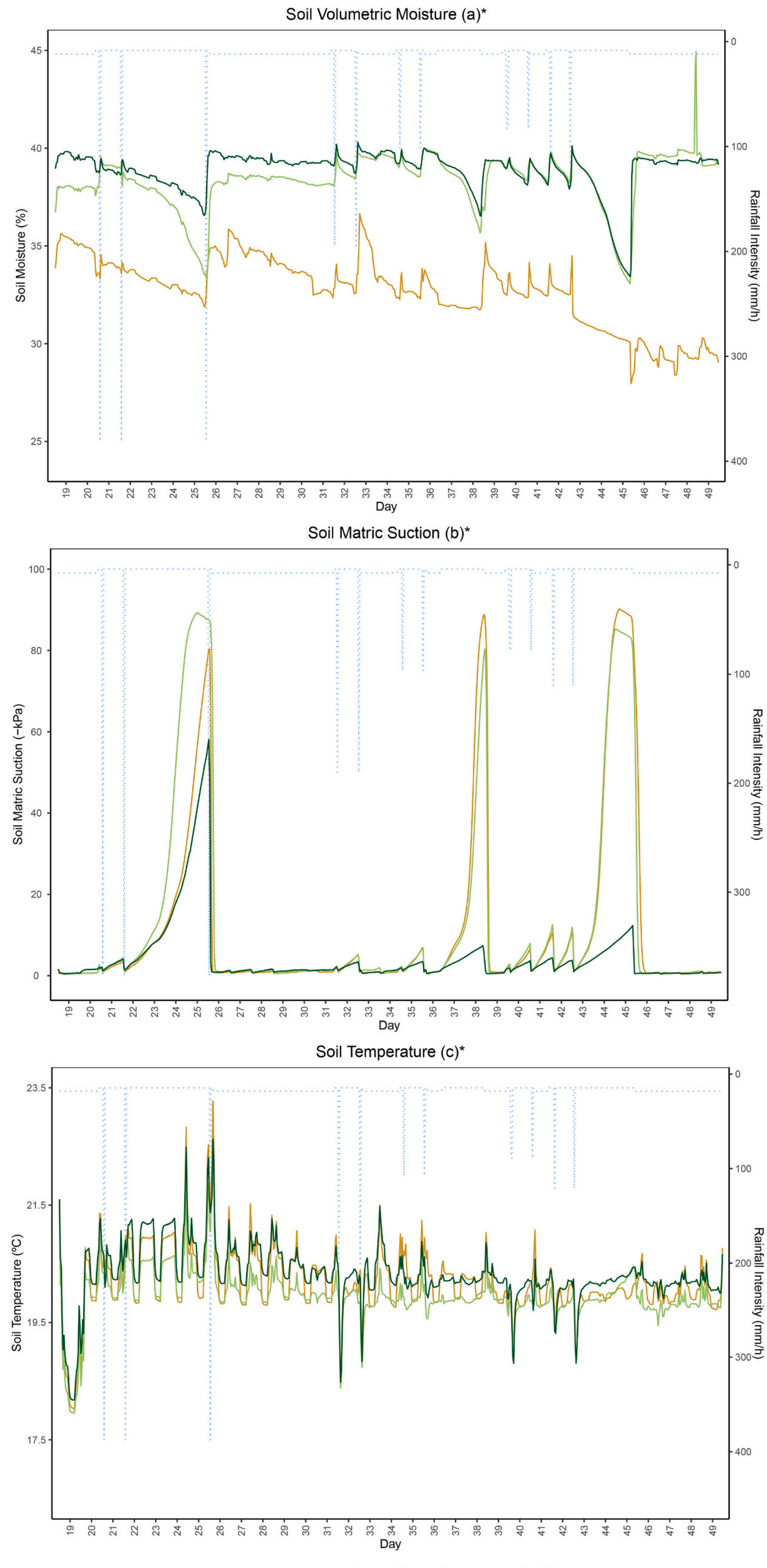

Fig. 8. Time series of the soil-water dynamics. (a) Hourly volumetric soil moisture content (θ; %); (b) Hourly soil matric suction (φ; -kPa); (c) Hourly soil temperature (t; °C). Time series recorded under the willow LPD (W), willow with alfalfa LPD (W + A), and fallow soil (C); and plotted together with simulated rainfall events (intensity; mm h^{-1}). * 0.01 level significant.

fostering biodiversity and plant succession dynamics (Key et al., 2022).

It is worth noting that the antecedent soil moisture was relevant in terms of the hydrological performance of the LPD (Fig. 7; Table 3; Schoener and Stone, 2019). In general, soil at water saturation level (scenario A; ScA) resulted in a higher subsurface flow and percolation when compared with soil at field capacity (scenario B; ScB; Fig. 7b-c; Table 3). This observation is likely to be related to the higher relative infiltration capacity of saturated soil e.g., Rodriguez-Iturbe and Porporato (2005). Within this context, soil at field capacity is expected to have a higher surface runoff due to its lower relative soil infiltration increasing the risk of flooding following a storm event (Lu and Likos, 2004). This behaviour was observed under the fallow treatment at dried soil conditions (ScB) but was not identified under the vegetated treatments (Fig. 7a; Table 3). This suggests that surface roughness and availability of channels for preferential flow and water infiltration created by vegetation had an impact in terms of stormwater runoff mitigation under drought conditions. Water retention was higher in soil at field capacity (ScB) compared to a wetted soil (ScA; Fig. 7d; Table 3). This implies that vegetated ground, which has roots and macropores that facilitate gravitational infiltration (Nachabe, 1995), can quickly reach field capacity and store and convey larger volumes of stormwater than fallow ground (Fig. 7d; Fig. 8a), thus positively impacting on the effectiveness of LPD to reduce slope instability and manage stormwater.

LPD treatments consistently showed higher soil moisture retention than fallow soil throughout the experiment (Fig. 8a). This can be attributed to the greater ability of vegetated soils to buffer moisture due to enhanced structure, organic matter, and microbiome (Gonzalez-Ollauri and Mickovski, 2020). These results suggest that LPD are highly effective at maintaining a soil-plant-atmosphere continuum under different soil hydrological conditions, as the retained soil moisture is likely to be available for plant water uptake and evapotranspiration in the event of absence of rainfall during summer or drought periods (Rodriguez-Iturbe and Porporato, 2005). Additionally, the shift in moisture content behaviour observed in the two vegetated treatments (noticeably lower moisture content in the W + A treatment after day 46, compared to the W treatment) may indicate that, as the root and shoot systems of the LPD and secondary species develop, their water uptake increases (Wang and Smith, 2004; Rodriguez-Iturbe and Porporato, 2005; Vetterlein and Doussan, 2016). This suggests that over time, after the initial establishment phase, LPD and the secondary plants can contribute to a decrease in moisture content through evapotranspiration during the vegetative season.

Although our research found that vegetation is crucial in maintaining consistent soil moisture levels (Fig. 8a), our observations of soil matric suction (Fig. 8b) do not align with this. Typically, an increase in vegetation structure (such as willow with alfalfa LPD; W + A) would result in greater plant water uptake and, subsequently, increased soil matric suction (Gonzalez-Ollauri and Mickovski, 2020). However, our findings suggest that W + A may retain more water due to changes in soil structure, leading to an overall increase in soil moisture content and a decrease in matric suction, while willow LPD (W) may retain water but also contribute to faster release, potentially due to poor soil structural changes (i.e., absence of alfalfa roots) and faster preferential flow through macropores (Bouma, 1981). The variations in soil matric suction between the vegetated treatments (W + A and W) were also noticeable during the three main soil drying periods (as shown in Fig. 8b). During the first drying peak, vegetation in both W and W + A was not well-developed, indicating that the presence of a secondary species (i.e., alfalfa) within the W + A treatment played an important role during the second and third soil drying conditions, maintaining a higher soil moisture content and lower soil matric suction compared to W treatment (Guo et al., 2019).

The highest levels of matric suction and temperature were observed in the fallow soil treatment (Fig. 8b-c), indicating that subsurface flow and water percolation may be limited (Fig. 7b-c; Table 3) due to higher soil density, lower roughness, and potential soil desiccation (Neumann et al., 2023). This behaviour, however, increases the risk of surface erosion and gully formation, which can ultimately lead to slope instability at first, and perhaps later as a shallow landslide (Gray and Sotir, 1996). Conversely, the vegetated treatments, which showed lower soil matric suction than the fallow soil (Fig. 8b), would also pose a risk to slope stability by accumulating water and increasing soil pore water pressures in the short term (Leung et al., 2015). This risk can be mitigated in the short term by the LPD itself, which would function in its civil engineering role (i.e., drainage, water conductivity; Campbell et al., 2008) up until the point when the LPD and the secondary plants are well-established. At this point, they take over the eco-hydrological functions such as land cover and surface roughness leading to a decrease in erosivity (Stokes et al., 2014); evapotranspiration leading to an increase in soil matric suction (Leung et al., 2015); root system morphology contributing to soil strength while ensuring continuity in water conductivity in the LPD (Wang et al., 2020); and regulation of soil temperature (Ni et al., 2019), minimising the possibility of slope instability in terms of erosion and shallow landslides.

It is acknowledged that minor inconsistencies and errors derived from the deployed setup and equipment may have affected the performance of the pilot laboratory experiment. During a storm simulation, leakages, changes in water pressure and partial water spray of the nozzles not reaching the columns, possibly impacted the volume of water inputs and thus on the soil-water mass balance (SWMB) components outputs, also leading to a few outliers (Fig. 7). However, while there were some water losses recorded during the study (Fig. 7e), we took these losses into account by incorporating them into the soil-water mass balance equation. Additionally, possible sensor malfunction led to anomalies within the soil-water volumetric content dataset, as observed on day 48 (Fig. 8a).

Further research is needed to understand when the hydrological performance of LPD is at its optimum, e.g., Wang et al. (2023). Furthermore, the observed behaviours on soil matric suction (i.e., similarities between willow LPD (W) and fallow soil (C)) and soil temperature (i.e., highest values under willow with alfalfa LPD (W + A) treatment, similar to fallow soil (C)) indicate the need for continuous monitoring of these parameters over an extended period. This would enable the identification of the critical point for the establishment of functional root and shoot systems (i.e., when these structures developed sufficiently to support the plant growth and survival through the roots' ability to absorb water and nutrients and the shoots' ability to photosynthesize and support aboveground growth; Rodriguez-Iturbe and Porporato, 2005) in both LPD and secondary plants when the differences between fallow soil and vegetated LPD become more pronounced.

Future studies could also quantify the evapotranspiration resulting from LPD as a forcing function removing water from the soil and contributing to the soil-plant-atmosphere balance (e.g., Gonzalez-Ollauri and Mickovski (2014) and Leung et al. (2015)). Additionally, the evidence gathered within this research needs to be validated by replicating the laboratory experiment. Ultimately, upscaling it to an open-air slope scale would ensure a higher degree of reliability since the variability of daily lighting and temperature, nocturnal fall humidity and capillary redistribution, presence of fauna, availability of explorable soil depth, water table, etc., could lead to substantial differences. It is also worth noting that the results found and explored herein are determined by the defined and applied LPD design and duration of the experiment (i.e., 52 days). Different designs (i.e., plant species, the overall size of the bundles, combined use of dead and live cuttings, etc.) and simulated environmental conditions (i.e., soil type, slope gradient, dormant season, etc.) could deliver different outputs. To gain a better understanding of the hydrological performance of LPD, it would be beneficial to conduct further numerical modelling studies (e.g., Elia et al., 2017). This approach would allow for a more detailed analysis and evaluation of the LPD effectiveness in preventing slope instability by slope drainage and stormwater management.

Nonetheless, the study presented herein can be a very solid starting point towards further understanding of the hydrological performance of LPD. This research was built upon an understudied field and successfully gathered base evidence on LPD effectiveness in draining sloped areas and managing stormwater. This allows further modelling performance and encourages LPD reproduction and upscaling for mitigation of slope instability risks.

5. Conclusions

This study provides a novel laboratory experiment to test the hydrological performance of LPD for slope drainage and stormwater management. It delivers an evidence base of this NbS supporting its adoption and upscaling for mitigation of slope instability risks. In light of our observations and findings, it can be concluded that:

- LPD have the potential to effectively manage stormwater reaching the slope by draining the excess stormwater runoff and attenuating water in the soil better than fallow soil. This was seen in the soil-water mass balance (SWMB) analysis, revealing the potential of LPD to drain but also to buffer moisture, delaying peak flows, and potentially making water available for the plants under drought periods;
- Subsurface flow and percolation are significantly higher under LPD treatments when compared to fallow ground. This is directly related to the presence of an enhanced structure in the soil (i.e., bundles of live cuttings and roots), which reinforces our hypothesis that LPD can be an effective NbS against erosion, shallow landslides, and flooding;
- LPD with a secondary plant species (i.e., alfalfa) results in a hydrological performance more beneficial to slope stability when compared to a willow LPD alone due to its higher surface roughness and enhanced number of micropores and channels for preferential flow;
- Antecedent soil moisture impacts on the hydrological performance of LPD by altering the relative infiltration capacity of the soil and by modifying the availability of channels for preferential flow.

In this paper, we have identified the aspects that deserve further consideration regarding the hydrological performance of LPD in connection to the onset of slope instability. We encourage replication of the laboratory experiment as means to validate the evidence presented as well as further investigation of LPD under different scales, designs, and environmental conditions (i.e., plant species, overall size of the bundles, soil type, slope gradient, etc.).

CRediT authorship contribution statement

Fernanda Berlitz: Writing – review & editing, Writing – original draft, Visualization, Methodology, Investigation, Formal analysis, Conceptualization. **Eefje Benschop:** Methodology, Investigation, Conceptualization. **Slobodan B. Mickovski:** Writing – review & editing, Supervision, Conceptualization. **Alejandro Gonzalez-Ollauri:** Writing – review & editing, Supervision, Conceptualization.

Declaration of competing interest

The authors declare that they have no known competing financial interests or personal relationships that could have appeared to influence the work reported in this paper.

Data availability

Data will be made available on request.

Acknowledgement

This research was funded by the European Education and Culture Executive Agency (EACEA) through an Erasmus Mundus Joint Master's Degree programme (Master of Urban Climate and Sustainability - www.murcs.eu; Grant No: 2017-1926), coordinated by the Glasgow Caledonian University. We also acknowledge the contributions of Lucie Podevin and Camille Grauby during data collection of our experiment.

Appendix A. Supplementary data

Supplementary data to this article can be found online at https://doi.org/10.1016/j.ecoleng.2024.107360.

References

Bodner, G., Leitner, D., Kaul, H.P., 2014. Coarse and fine root plants affect pore size distributions differently. Plant Soil 380 (1), 133–151. https://doi.org/10.1007/s11104-014-2079-8.

Bouma, J., 1981. Soil morphology and preferential flow along macropores. J. Agric. Water Manag. 3, 235–250. https://doi.org/10.1016/0378-3774(81)90009-3.

Box, J.M.M., Carmona, J.N. (Eds.), 2005. Prontuario de Agricultura: Cultivos Agrícolas. Ediciones Mundi-Prensa, Madrid, Spain. ISBN 13:9788484762485.

Campbell, S.G., Shaw, R., Sewell, R., Wong, J., 2008. Guidelines for Soil Bioengineering Applications on Natural Terrain Landslide Scars. Geotechnical Engineering Office, Hong Kong.

Elia, G., Cotecchia, F., Pedone, G., Vaunat, J., Vardon, P.J., Pereira, C., Springman, S.M., Rouainia, M., Van Esch, J., Koda, E., Josifovski, J., Nocilla, A., Askarinejad, A., Stirling, R., Helm, P., Lollino, P., Osinski, P., 2017. Numerical modelling of slope–vegetation–atmosphere interaction: an overview. Q. J. Eng. Geol. Hydrogeol. 50, 249–270. https://doi.org/10.1144/qjegh2016-079.

Fleming, G., 2002. Learning to live with rivers - the ICE's report to government. Civ. Eng. 150 (5), 15–21. https://doi.org/10.1680/cien.2002.150.5.15.

Gerten, D., Schaphoff, S., Haberlandt, U., Lucht, W., Sitch, S., 2004. Terrestrial vegetation and water balance — hydrological evaluation of a dynamic global vegetation model. J. Hydrol. 286, 249–270. https://doi.org/10.1016/j.jhydrol.2003.09.029.

Ghestem, M., Sidle, R.C., Stokes, A., 2011. The influence of plant root systems on subsurface flow: implications for slope stability, 61 (11), 869–879. https://doi.org/10.1525/bio.2011.61.11.6.

Gonzalez-Ollauri, A., Mickovski, S.B., 2014. Integrated model for the hydro-mechanical effects of vegetation against shallow landslides. EQA - Int. J. Environ. Qual. 13 (13), 37–59. https://doi.org/10.6092/issn.2281-4485/4535.

Gonzalez-Ollauri, A., Mickovski, S.B., 2016. Using the root spread information of pioneer plants to quantify their mitigation potential against shallow landslides and erosion in temperate humid climates. Ecol. Eng. 95, 302–315. https://doi.org/10.1016/j.ecoleng.2016.06.028.

Gonzalez-Ollauri, A., Mickovski, S.B., 2017a. Hydrological effect of vegetation against rainfall-induced landslides. J. Hydrol. 549, 374–387. https://doi.org/10.1016/j.jhydrol.2017.04.014.

Gonzalez-Ollauri, A., Mickovski, S.B., 2017b. Plant-best: a novel plant selection tool for slope protection. Ecol. Eng. 106, 154–173. https://doi.org/10.1016/j.ecoleng.2017.04.066.

Gonzalez-Ollauri, A., Mickovski, S.B., 2020. The effect of willow (Salix sp.) on soil moisture and matric suction at a slope scale. Sustainability (Switzerland) 12 (23), 1–19. https://doi.org/10.3390/su12239789.

Gonzalez-Ollauri, A., Mickovski, S.B., Anderson, C.C., Debele, S., Emmanuel, R., Kumar, P., Loupis, M., Ommer, J., Pfeiffer, J., Panga, D., Pilla, F., Sannigrahi, S., Toth, E., Ukonmaanaho, L., Zieher, T., 2023. A nature-based solution selection framework: criteria and processes for addressing hydro-meteorological hazards at open-air laboratories across Europe. J. Environ. Manag. 331 (117183), 1–12. https://doi.org/10.1016/j.jenvman.2022.117183.

Gray, D., Sotir, R., 1996. Biotechnical Soil Bioengineering Slope Stabilization: A Practical Guide for Erosion Control. John Wiley & Sons, New York, US.

Guo, L., Liu, Y., Wu, G., Huang, Z., Cui, Z., Cheng, Z., Zhang, R., 2019. Preferential water flow: influence of alfalfa (Medicago sativa L.) decayed root channels on soil water infiltration. J. Hydrol. 578, 1–8. https://doi.org/10.1016/j.jhydrol.2019.124019.

Jørgensen, S.E., Fath, B.D. (Eds.), 2011. Fundamentals of Ecological Modelling. Elsevier, Amsterdam, NL. ISBN 9780444535672.

Key, I.B., Smith, A.C., Turner, B., Chausson, A., Girardin, C.A.J., Macgillivray, M., Seddon, N., 2022. Biodiversity outcomes of nature-based solutions for climate change adaptation: characterising the evidence base. Front. Environ. Sci. 10, 1–29. https://doi.org/10.3389/fenvs.2022.905767.

Kim, J.H., Fourcaud, T., Jourdan, C., Maeght, J.-L., Mao, Z., Metayer, J., Meylan, L., Pierret, A., Rapidel, B., Roupsard, O., de Rouw, A., Snachez, M.V., Wang, Y., Stokes, A., 2017. Vegetation as a driver of temporal variations in slope stability: the impact of hydrological processes. Geophys. Res. Lett. 44, 4897–4907. https://doi.org/10.1002/2017GL073174.

Kruskal, W.H., Wallis, W.A., 1952. Use of ranks in one-criterion variance analysis. J. Am. Stat. Assoc. 47, 583–621.

Kuehler, E., Hathaway, J., Tirpak, A., 2017. Quantifying the benefits of urban forest systems as a component of the green infrastructure stormwater treatment network. Ecohydrology 10 (e1813), 1–10. https://doi.org/10.1002/eco.1813.
Leung, A.K., Garg, A., Ng, C.W.W., 2015. Effects of plant roots on soil-water retention and induced suction in vegetated soil. Eng. Geol. 193, 183–197. https://doi.org/10.1016/j.enggeo.2015.04.017.
Li, X., Zhang, L., Zhang, Z., 2006. Soil bioengineering and the ecological restoration of riverbanks at the Airport Town, Shanghai, China. Ecol. Eng. 26 (3), 304–314. https://doi.org/10.1016/j.ecoleng.2005.10.011.
Li, J., Cui, P., Yin, Y., 2023. Field observation and micro-mechanism of roots-induced preferential flow by infiltration experiment and phase-field method. J. Hydrol. 623 (129756), 1–13. https://doi.org/10.1016/j.jhydrol.2023.129756.
Liu, H.W., Feng, S., Ng, C.W.W., 2016. Analytical analysis of hydraulic effect of vegetation on shallow slope stability with different root architectures. Comput. Geotech. 80, 115–120. https://doi.org/10.1016/j.compgeo.2016.06.006.
Lokhorst, I.R., de Lange, S.I., van Buiten, G., Selaković, S., Kleinhans, M.G., 2019. Species selection and assessment of eco-engineering effects of seedlings for biogeomorphological landscape experiments. Earth Surf. Process. Landf. 44, 2922–2935. https://doi.org/10.1002/esp.4702.
Lu, N., Likos, W.J., 2004. Unsaturated Soil Mechanics. John Wiley & Sons, New Jersey, US.
Lu, J., Zhang, Q., Werner, A.D., Li, Y., Jiang, S., Tan, Z., 2020. Root-induced changes of soil hydraulic properties – a review. J. Hydrol. 589 (125203), 1–13. https://doi.org/10.1016/j.jhydrol.2020.125203.
Mickovski, S.B., 2021. Re-thinking soil bioengineering to address climate change challenges. Sustainability 13 (6), 14. https://doi.org/10.3390/su13063338.
Mickovski, S.B., van Beek, L.P.H., 2009. Root morphology and effects on soil reinforcement and slope stability of young vetiver (Vetiveria zizanioides) plants grown in semi-arid climate. Plant Soil 324 (1), 43–56. https://doi.org/10.1007/s11104-009-0130-y.
Miller, J.D., Vesuviano, G., Wallbank, J.R., Fletcher, D.H., Jones, L., 2023. Landscape and urban planning hydrological assessment of urban nature-based solutions for urban planning using ecosystem service toolkit applications. Landsc. Urban Plan. 234 (104737), 1–12. https://doi.org/10.1016/j.landurbplan.2023.104737.
Mitchell, A.R., Ellsworth, T.R., Meek, B.D., 1995. Effect of root systems on preferential flow in swelling soil. Commun. Soil Sci. Plant Anal. 26 (15–16), 2655–2666. https://doi.org/10.1080/00103629509369475.
Nachabe, M.H., 1995. Estimating hydraulic conductivity for models of soils with macropores. J. Irrig. Drain. Eng. 121 (1), 95–102. https://doi.org/10.1061/(ASCE)0733-9437(1995)121:1(95).
Neumann, M., Kavka, P., Tejkl, A., Laburda, T., Beck-Broichsitter, S., 2023. Influence of soil cover on surface runoff, infiltration, and percolation. In: EGU General Assembly 2023, Vienna, Austria, 24–28 Apr 2023, EGU23-5351. https://doi.org/10.5194/egusphere-egu23-5351.
Ni, J., Cheng, Y., Wang, Q., Wang, C., Ng, W., Garg, A., 2019. Effects of vegetation on soil temperature and water content: field monitoring and numerical modelling. J. Hydrol. 571, 494–502. https://doi.org/10.1016/j.jhydrol.2019.02.009.
Norris, J.E., Stokes, A., Mickovski, S.B., Cammeraat, E., Beek, R., Nicoll, B.C., Achim, A. (Eds.), 2008. Slope Stability and Erosion Control: Ecotechnological Solutions. Springer, Dordrecht, NL. https://doi.org/10.1007/978-1-4020-6676-4.
Panagos, P., De Rosa, D., Liakos, L., Labouyrie, M., Borrelli, P., Ballabio, C., 2024. Soil bulk density assessment in Europe. Agric. Ecosyst. Environ. 364 (108907), 1–14. https://doi.org/10.1016/j.agee.2024.108907.
Polster, D.F., 1989. Successional reclamation in western Canada: New light on an old subject. American Society of Mining and Reclamation, pp. 333–338. https://doi.org/10.21000/jasmr89010333. January 1989.
Pratt, J.W., Gibbons, J.D., 1981. Kolmogorov-Smirnov two-sample tests. In: Concepts of Nonparametric Theory. Springer Series in Statistics, New York, US.
Recking, A., Piton, G., Montabonnet, L., Posi, S., Evette, A., 2019. Design of fascines for riverbank protection in alpine rivers: insight from flume experiments. Ecol. Eng. 138, 323–333. https://doi.org/10.1016/j.ecoleng.2019.07.019.
Rodriguez-Iturbe, I., Porporato, A., 2005. Ecohydrology of water-controlled ecosystems: Soil moisture and plant dynamics. In: Ecohydrology of Water-Controlled Ecosystems: Soil Moisture and Plant Dynamics, vol. 9780521819. Cambridge University Press, New York, US. https://doi.org/10.1017/CBO9780511535727.
Schiechtl, H., Stern, R., 1997. In: Barker, D.H. (Ed.), Water Bioengineering Techniques for Watercourse, Bank and Shoreline Protection. Blackwell Science, UK. ISBN 0632040661.
Schoener, G., Stone, M.C., 2019. Impact of antecedent soil moisture on runoff from a semiarid catchment. J. Hydrol. 569, 627–636. https://doi.org/10.1016/j.jhydrol.2018.12.025.
Scottish Government, 2021. Water-Resilient Places: A Policy Framework for Surface Water Management and Blue-Green Infrastructure. Water Industry and Flood Risk Management Teams, UK. ISBN 9781800046139.
Scottish Water, 2018. Sewers for Scotland v4.0. Scottish Water and WRc plc, UK.
Shaw, E.M., Beven, K.J., Chappell, N.A., Lamb, R., 2017. Hydrology in Practice, 4th ed. CRC Press, UK. ISBN 9780415370424.
Sidle, R.C., Bogaard, T.A., 2016. Dynamic earth system and ecological controls of rainfall-initiated landslides. Earth Sci. Rev. 159, 275–291. https://doi.org/10.1016/j.earscirev.2016.05.013.
Sotir, R., Fischenich, C., 2001. EMRRP Technical Notes Collection (ERDC TN-EMRRP-SR-31): Live and Inert Fascine Streambank Erosion Control. US Army Engineer Research and Development Center, Vicksburg, US.
Stokes, A., Douglas, G.B., Fourcaud, T., Giadrossich, F., Gillies, C., Hubble, T., Kim, J.H., Loades, K.W., Mao, Z., McIvor, I.R., Mickovski, S.B., Mitchell, S., Osman, N., Phillips, C., Poesen, J., Polster, D., Preti, F., Raymond, P., Rey, F., Schwarz, M., Walker, L.R., 2014. Ecological mitigation of hillslope instability: ten key issues facing researchers and practitioners. Plant Soil 377 (1–2), 1–23. https://doi.org/10.1007/s11104-014-2044-6.
UKCEH, 1999. Flood Estimation Handbook. UK Centre for Ecology & Hydrology, Wallingford.
Vetterlein, D., Doussan, C., 2016. Root age distribution: how does it matter in plant processes? A focus on water uptake. Plant Soil 407, 145–160. https://doi.org/10.1007/s11104-016-2849-6.
Wang, E., Smith, C.J., 2004. Modelling the growth and water uptake function of plant root systems: a review. Aust. J. Agric. Res. 55, 501–523. https://doi.org/10.1071/AR03201.
Wang, X., Ma, C., Wang, Y., Wang, Y., Li, T., Dai, Z., Li, M., 2020. Effect of root architecture on rainfall threshold for slope stability: variabilities in saturated hydraulic conductivity and strength of root-soil composite. Landslides 17, 1965–1977. https://doi.org/10.1007/s10346-020-01422-6.
Wang, M., Liu, M., Zhang, D., Qi, J., Fu, W., Zhang, Y., Rao, Q., Bakhshipour, A.E., Tan, S. K., 2023. Assessing and optimizing the hydrological performance of Grey-Green infrastructure systems in response to climate change and non-stationary time series. Water Res. 232 (119720), 1–12. https://doi.org/10.1016/j.watres.2023.119720.
Yao, C., Lu, C., Chen, K., Wang, C., Wang, H., Wu, F., 2023. The contribution rate of stem-leaf and root of alfalfa (Medicago sativa L.) to sediment and runoff reduction. Land Degrad. Dev. 34, 3991–4005. https://doi.org/10.1002/ldr.4731.
Zha, X., Luo, P., Zhu, W., Wang, S., Lyu, J., Zhou, M., Huo, A., Wang, Z., 2021. A bibliometric analysis of the research on Sponge City: current situation and future development direction. Ecohydrology 14 (7), 1–16. https://doi.org/10.1002/eco.2328.
Zhang, Y., Wang, L., Zhang, W., Zhang, Z., Zhang, M., 2023. Quantification of root systems and soil macropore networks association to soil saturated hydraulic conductivity in forested wetland soils. Forests 14 (132), 1–16. https://doi.org/10.3390/f14010132.